



## On-off-on fluorescence detection for biomolecules by a fluorescent cage through host-guest complexation in water



Honghong Duan<sup>a</sup>, Fan Cao<sup>a</sup>, Minjie Zhang<sup>b</sup>, Meng Gao<sup>b</sup>, Liping Cao<sup>a,\*</sup>

<sup>a</sup> College of Chemistry and Materials Science, Northwest University, Xi'an 710069, China

<sup>b</sup> National Engineering Research Center for Tissue Restoration and Reconstruction, Key Laboratory of Biomedical Engineering of Guangdong Province, Key Laboratory of Biomedical Materials and Engineering of the Ministry of Education, Innovation Center for Tissue Restoration and Reconstruction, South China University of Technology, Guangzhou 510006, China

### ARTICLE INFO

#### Article history:

Received 6 September 2021

Revised 26 October 2021

Accepted 2 November 2021

Available online 10 November 2021

#### Keywords:

Host-guest complexation

Tetraphenylethene-based octacationic cage

Nucleoside derivatives

Fluorescence

Cell imaging

### ABSTRACT

Detection of nucleoside derivatives has paramount importance because they are the essential biomolecular units for all life. Herein, we report a host-guest approach by using a fluorescent tetraphenylethene-based octacationic cage as host and 8-hydroxypyrene-1,3,6-trisulfonic acid trisodium salt (HPTS) as guest and fluorescent indicator to form non-fluorescent 1:1:1 host-(*endo-exo*)guest complex in water. This new host-(*endo-exo*)guest complex can be successfully used for detecting nucleosides (e.g., ATP and GTP), DNA (e.g., sm-DNA), and antibiotics (e.g., Penicillin G) with off-on fluorescence response via a competitive host-guest exchange with HPTS as *exo*-guest in water. Furthermore, this on-off-on fluorescent host-guest complex is also used for cell imaging based on ATP concentration in HeLa cells. Therefore, this study not only provides insight into the construction of a supramolecular probe with on-off-on fluorescence via host-guest complexation and exchange in solution, but also realizes a universal method for detecting and monitoring biomolecules.

© 2021 Published by Elsevier B.V. on behalf of Chinese Chemical Society and Institute of Materia Medica, Chinese Academy of Medical Sciences.

The research progress of fluorescence detection systems for biomolecules has received considerable attention in recent years because of the important application in a wide range of fields such as biology, chemical process, and environmental science [1–5]. Specifically, nucleoside derivatives, such as ATP, CTP, GTP and UTP, are essential in the regulation of organisms [6–10]. They are not only the raw materials for RNA synthesis, but also play an important role in metabolism process. For example, ATP is the "electricity" in organisms; GTP is essential in protein synthesis; UTP is involved in carbohydrate metabolism in organisms; CTP plays an important role in phospholipid synthesis [11,12]. However, owing to the solvation of phosphate and sugar groups and the competitive hydrogen bonding of base units with water molecules, their detection and recognition in the aqueous medium still are limited [13–15]. On the other hand, most of conventional fluorescent probes exhibit aggregation-caused quenching (ACQ) in water when aggregating and/or binding with biomolecules, which often makes the detection process to employ a fluorescent "turn-off" feature with the high background noise and poor sensitivity [16]. There-

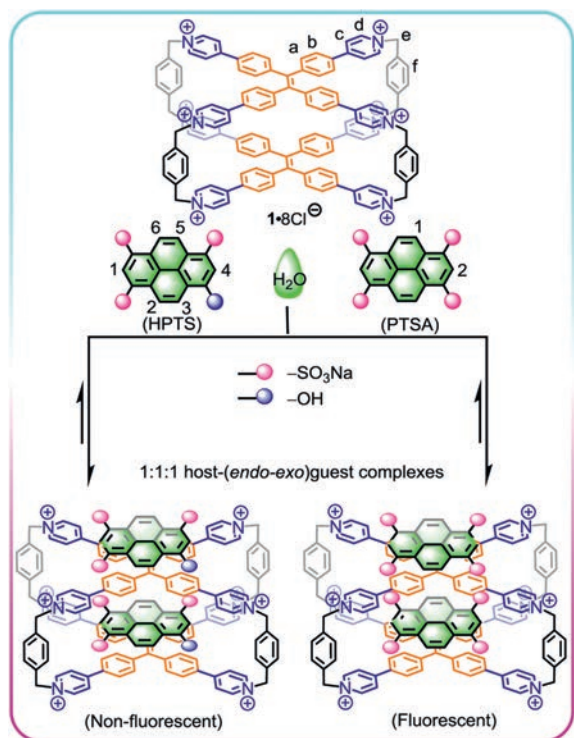
fore, the use of fluorescent turn-on mechanism can provide a better approach for the detection of biomolecules.

In host-guest chemistry, a variety of macrocyclic hosts, such as crown ethers [17,18], cyclodextrins [19,20], calix[n]arenes [21,22], pillar[n]arenes [23,24], cyclophanes [25,26], cucurbit[n]urils [27,28], and molecular cages [29–36], have been synthesized and their functions have been widely investigated for molecular recognition, drug delivery systems, photoelectric materials, and supramolecular polymers. Especially, molecular cages with various sizes, shapes, and functional groups have been widely developed, because of not only their unique hydrophobic cavity for selectively binding guest molecules but also their reduction-oxidation properties for electronic devices (e.g., semiconductor) and molecular machines (e.g., molecular shuttle and molecular pump) [37–39]. Furthermore, molecular cages have also attracted intensive attention for biochemical applications including bioimaging and drug/gene delivery [40–44], photodynamic therapy [45,46], and biosensors [47].

Recently, we have utilized tetraphenylethene (TPE) and pyridinium units as molecular building blocks to construct a series of supramolecular hosts including macrocycles, cages, and frameworks, which exhibited promising applications in host-guest recognitions, light-harvesting systems, and stimuli-responsive fluorescent materials [48–59]. Specially, combined with the physicochem-

\* Corresponding author.

E-mail address: [chcaoliping@nwu.edu.cn](mailto:chcaoliping@nwu.edu.cn) (L. Cao).



**Scheme 1.** The formation of host-(*endo-exo*)guest complexes between  $1-8Cl^-$  and HPTS/PTSA.

ical properties of TPE and pyridinium units, the tetraphenylethene-based octacationic cage ( $1-8Cl^-$ , Scheme 1) possesses a large and rigid binding cavity, positive-charged surfaces, good water-solubility, and excellent fluorescence [52]. This fluorescent cationic cage exhibits remarkable affinities toward negative-charged chiral biomolecules *via* a series of CH- $\pi$ ,  $\pi$ - $\pi$ , hydrophobic, and electrostatic interactions in water to achieve conformationally adaptive chirality with circular dichroism (CD) and circularly polarized luminescence (CPL) responses [57]. As a result, this cage is endowed with several features, such as host-guest ability, strong fluorescence, and good water-solubility, which make it well suited for studying stimuli-responsive fluorescence processes through forming host-guest complexes with organic dyes in aqueous media. Two water-soluble pyrene-based dyes, 8-hydroxypyrene-1,3,6-trisulfonic acid trisodium salt (HPTS) and 1,3,6,8-pyrenetetrasulfonic acid tetrasodium salt (PTSA), are selected as guest to form fluorescent host-guest complexes with  $1-8Cl^-$  in water. Herein, we report a host-guest approach by using a tetraphenylethene-based octacationic cage as host and HPTS as guest to form non-fluorescent 1:1:1 host-(*endo-exo*)guest complexes, which is successfully used for detecting nucleosides (e.g., ATP and GTP), DNA (e.g., sm-DNA), and antibiotics (e.g., Penicillin G) with turn-on fluorescence response *via* a competitive host-guest exchange with *exo*-HPTS in water. Furthermore, this on-off-on fluorescent host-guest complex also is used for cell imaging based on ATP concentration in HeLa cells.

Initially, the host-guest complexation between  $1-8Cl^-$  and HPTS was investigated by employing NMR experiments. The  $^1H$  NMR titration of  $1-8Cl^-$  with HPTS showed the following changes for the proton resonances of both cage and guest (Fig. 1a): 1) With the gradual addition of HPTS, the proton resonances ( $H_d$ - $H_c$ ) of pyridinium rings showed downfield shifts while the proton resonances ( $H_a$ - $H_b$ ) in the central part of the TPE faces displayed different upfield shifts which caused by  $\pi$ -electron deshielding and shielding of HPTS. 2) The proton resonances ( $H_1$ - $H_6$ ) corre-

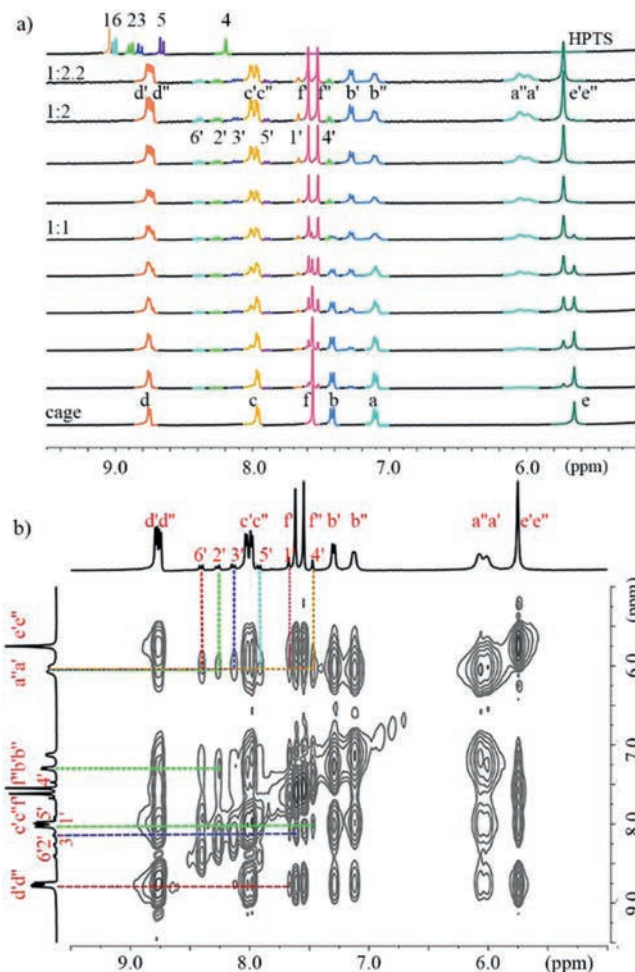


**Fig. 1.** (a)  $^1H$  NMR titration (400 MHz, 298 K,  $D_2O$ ) of  $1-8Cl^-$  (0.4 mmol/L) titrated with HPTS (0–2.2 equiv.). Here, primes ' and ' ' denote the resonances of the inner and outer tetrapyrindinium-TPE surfaces within the 1:1:1 host-(*endo-exo*)guest complex, respectively. (b) NOESY spectrum recorded (400 MHz, 298 K,  $D_2O$ ) for  $1-8Cl^-$  (2.0 mmol/L) with HPTS (2.0 equiv.).

sponding to HPTS shifted upfield, strongly confirming that HPTS molecules are completely encapsulated inside the cavity of cage to form the host-guest inclusion complex. 3) The addition of 2.0 equiv. of HPTS induced that all resonances ( $H_a$ - $H_f$ ) of cage split into two sets of peaks ( $H_a'$ - $H_f'$  and  $H_a''$ - $H_f''$ ), because the formation of a new host-(*endo-exo*)guest complex decreases the symmetry of cage. Based on the results from NMR, the cavity of cage cannot encapsulate two HPTS. Therefore, one HPTS molecule as *endo*-guest is located inside the cavity of cage *via*  $\pi$ - $\pi$ , hydrophobic, and electrostatic interactions, and another HPTS molecule as *exo*-guest binds on the tetrapyrindinium-TPE surface to give a 1:1:1 host-(*endo-exo*)guest complex ( $1 \supset \text{endo-HPTS}$ )-*exo*-HPTS *via* electrostatic interactions between the positive-charged surface of cage and the negative-charged sulfonic groups of HPTS.

Furthermore,  $^1H$ - $^1H$  correlation spectroscopy (COSY) spectra show strong signal peaks between  $H_a'$  and  $H_b'$ , and  $H_a''$  and  $H_b''$ , which indicates that the symmetry of the cage is broken and the 1:1:1 host-(*endo-exo*)guest complex is formed (Fig. S1 in Supporting information). Besides, nuclear overhauser effect spectroscopy (NOESY) spectra showed the correlation signals between proton  $H_1'$ - $H_6'$  of HPTS and proton  $H_a'$ - $H_d'$  on the TPE units of cage (Fig. 1b), indicating that HPTS and cage form host-guest complex. The single host-guest complex was confirmed by diffusion-ordered spectroscopy (DOSY), which showed a similar diffusion co-

efficient  $[(1.79 \pm 0.03) \times 10^{-10} \text{ m}^2/\text{s}]$  when compared with that of  $1\text{-}8\text{Cl}^-$   $[(1.95 \pm 0.05) \times 10^{-10} \text{ m}^2/\text{s}]$  in  $\text{D}_2\text{O}$  at 298 K (2.0 mmol/L), thus suggesting the formation of a host-guest complex (Figs. S2 and S3 in Supporting information). On the other hand, electrospray ionization time-of-flight mass spectrometry (ESI-TOF-MS) provided further evidence for  $1\text{-}8\text{Cl}^-:\text{HPTS} = 1:2$  (including inner and outer guests) with continuous charge states at  $m/z$  663.6344, 896.5014, and 877.1946 corresponding to +4 to +3 charge states due to successive loss of the  $\text{Cl}^-$  and  $\text{Na}^+$  counterions. Meanwhile,  $1\text{-}8\text{Cl}^-:\text{HPTS} = 1:1$  with continuous charge states at  $m/z$  430.5416, 547.1665, 741.2040 and 1129.7878 corresponding to +5 to +2 charge states due to successive loss of the  $\text{Cl}^-$  and  $\text{Na}^+$  counterions (Figs. S4 and S5 in Supporting information). Owing to the weak binding between cage and *exo*-HPTS, only one binding constant between  $1\text{-}8\text{Cl}^-$  and *endo*-HPTS was estimated as  $(1.85 \pm 0.13) \times 10^5 \text{ L/mol}$  by UV-titration experiment (Fig. S6 in Supporting information).

Next, the host-guest behavior of  $1\text{-}8\text{Cl}^-$  and PTSA was investigated in  $\text{D}_2\text{O}$ . In  $^1\text{H}$  NMR titration of  $1\text{-}8\text{Cl}^-$  with PTSA, downfield shifts were observed for pyridinium protons ( $\text{H}_c'$ - $\text{H}_d'$ ), bridging  $\text{CH}_2$  groups ( $\text{H}_e'$ ), and *p*-xylylene moieties ( $\text{H}_f'$ ), while the phenyl proton resonances ( $\text{H}_a'$ - $\text{H}_b'$ ) located in the central part of the cage's TPE units showed apparent upfield shifts as compared to the free cage at 1:1 ratio, which caused by  $\pi$ -electron deshielding and shielding of PTSA (Fig. S7 in Supporting information). Meanwhile, proton resonances ( $\text{H}_1$ - $\text{H}_2$ ) showed obvious upfield shifts and was split indicating that PTSA was entirely located within the cage and shielded by the cavity of  $1\text{-}8\text{Cl}^-$ . Furthermore, NOE correlation signals were observed between proton  $\text{H}_1'$ - $\text{H}_2'$  of PTSA and proton  $\text{H}_a'$ - $\text{H}_b'$  on the TPE of cage from the 2D NOESY NMR spectrum. These results further confirm the central location of PTSA in the cage cavity (Fig. S8 in Supporting information). However, with the gradual addition of PTSA, a lot of precipitate began to appear, and when 2.0 equiv. of PTSA was added, host-guest complex was completely precipitated, resulting in the complete disappearance of NMR signal. We speculated that two PTSA with eight negative sulfonic groups and octacationic cage form a poor water-soluble zwitterionic complex ( $1\text{-}8\text{Cl}^-:\text{PTSA} = 1:2$ ) through multiple electrostatic interactions. ESI-TOF-MS further provided evidence for the formation of  $1\text{-}8\text{Cl}^-:\text{PTSA}$  with continuous charge states at  $m/z$  553.9076, 750.5335, corresponding to +4 to +3 charge states due to successive loss of the  $\text{Cl}^-$  and  $\text{Na}^+$  counterions (Fig. S9 in Supporting information). The binding constants between  $1\text{-}8\text{Cl}^-$  and PTSA was calculated as  $(8.01 \pm 0.09) \times 10^5 \text{ L/mol}$  for  $1\text{-}8\text{Cl}^-:\text{PTSA}$  (Fig. S10 in Supporting information).

Subsequently, the photophysical properties of  $1\text{-}8\text{Cl}^-$  with HPTS/PTSA were analyzed by fluorescence and UV-vis experiments in water. As shown in Fig. 2a, when HPTS was successively added into the solution of cage in water, the absorbance at 284 nm increased and red-shifted to 290 nm, while the absorbance at 362 nm decreased and red-shifted to 369 nm, indicating the formation of the host-guest complex. At the same time, the absorption peak from 440 nm gradually appears, which may be caused by a strong intermolecular charge-transfer interaction between anionic HPTS and octacationic pyridinium units of cage. A dramatic fluorescence quenching ( $\Phi_F =$  from 0.27 to  $<0.01$ ) of cage at 540 nm when 2.0 equiv. of HPTS was added, which could be attributed to the strong photoinduced electron transfer (PET) from HPTS to cage based on the formation of the host-guest complex (Fig. 2b and Table S1 in Supporting information) [60–62]. On the other hand, when PTSA was successively added to cage in water, UV-vis spectroscopy showed that there was weak charge transfer interaction between  $1\text{-}8\text{Cl}^-$  and PTSA (Fig. 2c). Therefore, compared with HPTS, the fluorescence spectra of PTSA showed different changes. With the gradual addition of PTSA, the fluorescence intensity of cage at 540

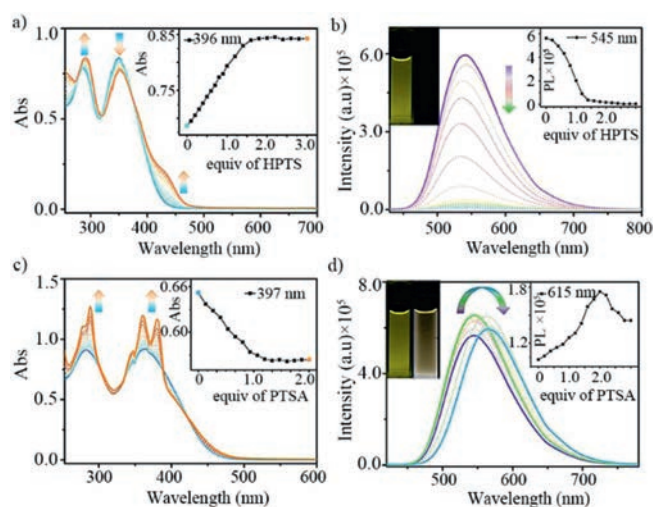
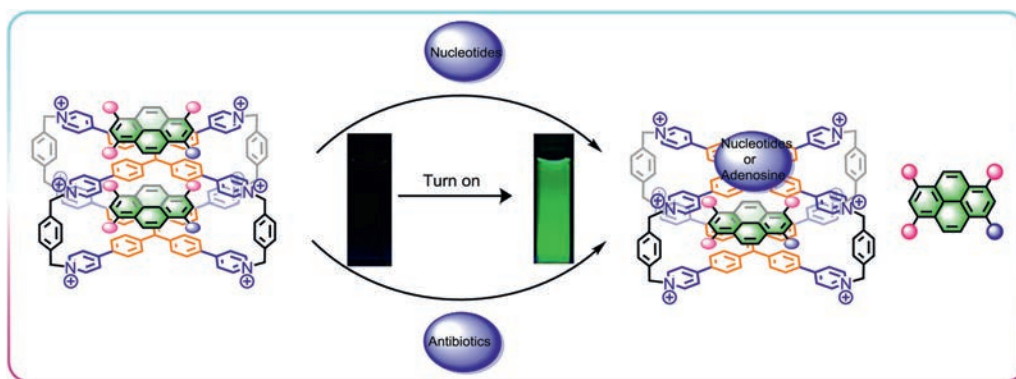


**Fig. 2.** (a) UV-vis and (b) fluorescence spectra of  $1\text{-}8\text{Cl}^-$  titrated with HPTS; (c) UV-vis and (d) fluorescence spectra of  $1\text{-}8\text{Cl}^-$  titrated with PTSA. [ $1\text{-}8\text{Cl}^-$ ] = 10  $\mu\text{mol/L}$ ,  $\lambda_{\text{ex}} = 410 \text{ nm}$ , Ex/Em slit = 1.2 nm, solvent:  $\text{H}_2\text{O}$ .

nm gradually increased and reached the maximum at 1:1 ratio, indicating that a 1:1 host-guest complex  $1\text{-}8\text{Cl}^-:\text{endo-PTSA}$  was formed, which is consistent with the result from NMR titration. The fluorescent enhancement could be contributed to the restriction of intramolecular rotation (RIR) of TPE units of cage when forming the host-guest complex. After the continuous addition of PTSA, the fluorescence intensity of cage showed red shift ( $\Delta\lambda_{\text{max}} = 23 \text{ nm}$ ) and slightly decreased (Fig. 2d), accompanying with a precipitation, indicating that a zwitterionic complex ( $1\text{-}8\text{Cl}^-:\text{endo-PTSA}:\text{exo-PTSA}$ ) was formed. The 1931 CIE chromaticity diagram also confirmed tracks of the fluorescence color change, followed by the titration of HPTS and PTSA (Fig. S11 in Supporting information).

Given the on-off fluorescence of octacationic cage with HPTS via host-(*endo*-*exo*)guest complexation, a series of negative-charged nucleoside derivatives (e.g., ATP, AMP, ADP, CTP, GTP and UTP, Scheme S1 in Supporting information) were selected as competitive guests for releasing the *exo*-HPTS from host-(*endo*-*exo*)guest complex ( $1\text{-}8\text{Cl}^-:\text{endo-HPTS}:\text{exo-HPTS}$ ) in aqueous solution. The competitive fluorescence experiments confirmed that the off-on fluorescence process can be realized by a competitive host-guest exchange, resulting different turn-on fluorescence responses for different nucleosides (Scheme 2). In fluorescence titration experiment (Fig. 3a), ( $1\text{-}8\text{Cl}^-:\text{endo-HPTS}:\text{exo-HPTS}$ ) exhibited various off-on fluorescence responses to nucleosides with different intensities, absolute quantum yields, and lifetimes (Table S1). Interestingly, the fluorescence titrations of ( $1\text{-}8\text{Cl}^-:\text{endo-HPTS}:\text{exo-HPTS}$ ) with ATP, GTP or UTP in water showed a drastic increase in the intensity of the emission of HPTS centered at 515 nm with high fluorescence intensity ratio ( $I/I_0$ ) of  $\sim 31$ ,  $\sim 71$  and  $\sim 25$ , respectively, exhibiting excellent green fluorescence emission of HPTS (Figs. 3a and b). However, other nucleosides, such as AMP, ADP, and CTP, just caused low enhancement in fluorescence intensity (Fig. 3b and Figs. S12–S17 in Supporting information). These results indicated that the electrostatic interaction between positive-charged pyridinium units of host and negative-charged phosphate groups of guests is main driving force to release the *exo*-HPTS from ( $1\text{-}8\text{Cl}^-:\text{endo-HPTS}:\text{exo-HPTS}$ ) via competitive host-guest exchange between the *exo*-HPTS of the host-guest complex and negative-charged nucleoside derivatives. For nucleoside derivatives with different nucleobase and the same number of phosphate groups, such as ATP, UTP, CTP and GTP, the fluorescence intensities of ( $1\text{-}8\text{Cl}^-:\text{endo-HPTS}:\text{exo-HPTS}$ ) were also different in the titration processes, which indicated that the nucleobase could also affect the



**Scheme 2.** Schematic illustration of the process of turn-on fluorescence via competitive exclusion host-guest exchange.

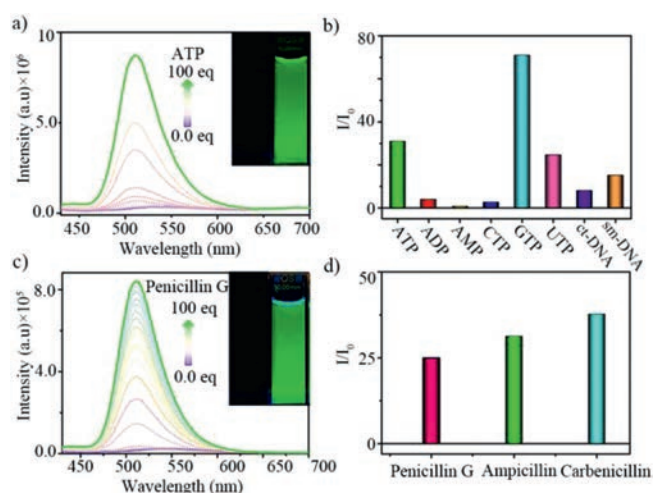


**Fig. 3.** Fluorescence spectra of ( $1\text{D-endo-HPTS-exo-HPTS}$ ) (10  $\mu\text{mol/L}$ ) titrated with (a) ATP (0–100.0 equiv.), (c) Penicillin G (0–100.0 equiv.). The  $I/I_0$  of ( $1\text{D-endo-HPTS-exo-HPTS}$ ) with (b) nucleosides and DNA (5.0 equiv.), (d) antibiotics (75.0 equiv.).

binding affinity with  $1\text{D-endo-HPTS}$  through hydrophobic effect and  $\pi$ - $\pi$  interaction.

To further verify the mechanism of turn-on fluorescence, NMR titration experiments were carried out in  $\text{D}_2\text{O}$ . When ATP was successively added to ( $1\text{D-endo-HPTS-exo-HPTS}$ ) in  $\text{D}_2\text{O}$ , the split proton peaks of **1** in ( $1\text{D-endo-HPTS-exo-HPTS}$ ) became broaden and converged again, indicating that the *exo*-HPTS on the outer surface was released after the addition of ATP (Fig. S18 in Supporting information). The *endo*-HPTS in the cavity still formed a stable host-guest inclusion complex with cage (Scheme 2). This experimental result is consistent with the fluorescence experiment.

Given the off-on fluorescence responses between ( $1\text{D-endo-HPTS-exo-HPTS}$ ) and nucleoside derivatives, ( $1\text{D-endo-HPTS-exo-HPTS}$ ) can be an ideal probe for DNA molecules. As expected, the addition of salmon testes DNA (smDNA) or calf thymus DNA (ctDNA) into the solution of ( $1\text{D-endo-HPTS-exo-HPTS}$ ) in water induced drastic fluorescence enhancement with  $\sim 8$  and  $\sim 15$  times, respectively (Fig. 3b and Figs. S19 and S20 in Supporting information). The detection limits of ( $1\text{D-endo-HPTS-exo-HPTS}$ ) were calculated to be 2.03  $\mu\text{g}/\mu\text{L}$  for smDNA and 1.53  $\mu\text{g}/\mu\text{L}$  for ctDNA, respectively (Figs. S19 and S20 in Supporting information).

With the abuse of antibiotics, the detection of antibiotics has become a hot spot for scientists (Scheme S1 in Supporting information). Due to the host-guest complex can detect negative-charged molecules with turn-on fluorescence response in water,

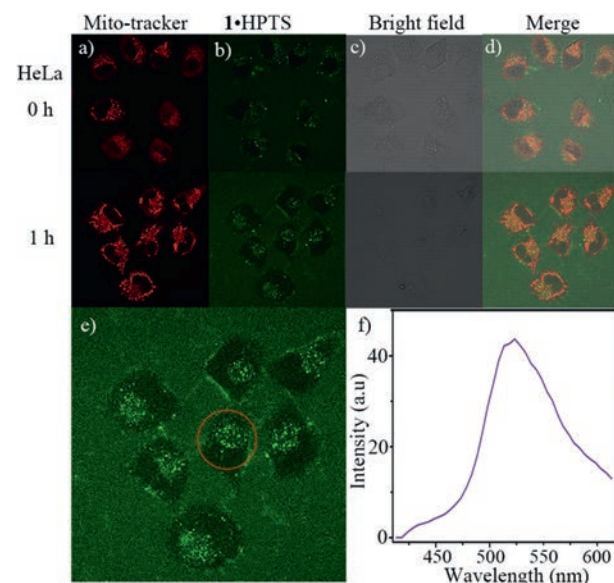


**Fig. 4.** CLSM imaging of HeLa cells stained with Mito-Tracker Deep Red (100  $\mu\text{mol/L}$ ) and ( $1\text{D-endo-HPTS-exo-HPTS}$ ) (50  $\mu\text{mol/L}$ ): (a) red channel, (b) green channel, (c) bright field, and (d) merged image. (e) CLSM imaging and (f) fluorescence intensity profile of regions of interest.

( $1\text{D-endo-HPTS-exo-HPTS}$ ) can be an ideal probe for antibiotics, such as Penicillin G, ampicillin and carbenicillin. Not surprisingly, with the addition of antibiotics, the emission intensity of ( $1\text{D-endo-HPTS-exo-HPTS}$ ) at 515 nm was significantly enhanced, with  $\sim 25$ ,  $\sim 31$  and  $\sim 38$  times (Figs. 3c and d Figs. S21–S23 in Supporting information), respectively. The off-on fluorescence response was successfully realized. These experimental results show that the host-(*endo-exo*)guest complex is universal and can be used as a probe to detect various substances in water.

The host-(*endo-exo*)guest complex ( $1\text{D-endo-HPTS-exo-HPTS}$ ) also was employed for cell imaging. Confocal laser scanning microscopy (CLSM) experiments in HeLa cells were performed to assess whether host-guest probe ( $1\text{D-endo-HPTS-exo-HPTS}$ ) could be in mitochondrion selectively, where the concentration of ATP is higher than other area in cells (Fig. 4). HeLa cells stained with Mito-Tracker Deep Red (a commercially mitochondrial tracker) displayed fluorescence on the red channel (Fig. 4a). The cells stained with ( $1\text{D-endo-HPTS-exo-HPTS}$ ) exhibited fluorescence on the green channel in Fig. 4b. The bright-field (Fig. 4c) and the merged (Fig. 4d) images of the cells showed overlap with commercial mitochondrial dyes, indicating that ( $1\text{D-endo-HPTS-exo-HPTS}$ ) can serve as a mitochondrion fluorescent probe. CLSM imaging and fluores-

cence intensity profile confirm that the emission is belonged to free HPTS (Figs. 4e and f).

In conclusion, we have reported the formation of 1:1:1 host-(endo-exo)guest complexes between TPE-based octacationic cage with organic dyes (e.g., HPTS and PSTA) in water. In these host-(endo-exo)guest complexes, cage can entirely encapsulate one dye as endo-guest inside the hydrophobic cavity and bind with another dye as exo-guest on the outer face through  $\pi$ - $\pi$ , hydrophobic, and electrostatic interactions. Their host-guest behaviours have been investigated by  $^1\text{H}$  NMR, UV-vis, fluorescence experiments. In aqueous media, cage exhibits an on-off fluorescence quenching when binding with HPTS. We utilize this on-off fluorescent host-guest system as a fluorescent probe to selectively detect negative-charged biomolecules including nucleoside derivatives, DNA, and antibiotics to achieve an off-on fluorescence response. We anticipate that this design of on-off-on fluorescent host-guest system has universality for probing biomolecules and cell imaging in water.

### Declaration of competing interest

The authors declare no conflict of interest.

### Acknowledgments

This work was supported by the National Natural Science Foundation of China (Nos. 22122108, 21971208 and 21771145), the Natural Science Basic Research Plan for Distinguished Young Scholars in Shaanxi Province of China (No. 2021JC-37), and the Fok Ying Tong Education Foundation (No. 171010).

### Supplementary materials

Supplementary material associated with this article can be found, in the online version, at doi:10.1016/j.ccl.2021.11.010.

### References

- [1] P.D. Beer, P.A. Gale, *Angew. Chem. Int. Ed.* 113 (2001) 502–532.
- [2] L.G. Fabbri, M. Licchelli, G. Rabaioli, A. Taglietti, *Coord. Chem. Rev.* 205 (2000) 85–108.
- [3] E.J. O'Neil, B.D. Smith, *Coord. Chem. Rev.* 250 (2006) 3068–3080.
- [4] T.Y. Liang, P.W. Yang, T.H. Wu, et al., *Chin. Chem. Lett.* 31 (2020) 2975–2979.
- [5] L. Wu, Y.S. Chen, J.F. Pei, et al., *Chin. J. Chem.* 37 (2019) 834–842.
- [6] S.C. McCleskey, M.J. Griffin, S.E. Schneider, J.T. McDevitt, E.V. Anslyn, *J. Am. Chem. Soc.* 125 (2003) 1114–1115.
- [7] L.M. Tumor, I. Piantanida, P. Novak, M. Zinic, *J. Phys. Org. Chem.* 15 (2002) 599–607.
- [8] S. Atilgan, E.U. Akkaya, *Tetrahedron Lett.* 45 (2004) 9269–9271.
- [9] J.Y. Kwon, N.J. Singh, H.N. Kim, et al., *J. Am. Chem. Soc.* 126 (2004) 8892–8893.
- [10] S.K. Kim, B.-S. Moon, J.H. Park, et al., *Tetrahedron Lett.* 46 (2005) 6617–6620.
- [11] W.N. Lipscomb, N. Strater, *Chem. Rev.* 96 (1996) 2375–2433.
- [12] D. Ramaiah, P.P. Neelakandan, A.K. Nair, R.R. Avirah, *Chem. Soc. Rev.* 39 (2010) 4158–4168.
- [13] N. Marcotte, A. Taglietti, *Supramol. Chem.* 15 (2003) 617–625.
- [14] A. Ojida, S. Park, Y. Mito-oka, I. Hamachi, *Tetrahedron Lett.* 43 (2002) 6193–6195.
- [15] J. Rebek, *Science* 235 (1987) 1478–1484.
- [16] D.J. Welsh, S.P. Jones, D.K. Smith, *Angew. Chem. Int. Ed.* 48 (2009) 4047–4051.
- [17] C.J. Pedersen, *J. Am. Chem. Soc.* 89 (1967) 2495.
- [18] G.W. Gokel, W.M. Leevy, M.E. Weber, *Chem. Rev.* 104 (2004) 2723–2750.
- [19] G. Crini, *Chem. Rev.* 114 (2014) 10940–10975.
- [20] J.J. Li, Y. Chen, J. Yu, N. Cheng, Y. Liu, *Adv. Mater.* 29 (2017) 1701905.
- [21] D.-S. Guo, Y. Liu, *Acc. Chem. Res.* 47 (2014) 1925–1934.
- [22] Z.Z. Lai, T. Zhao, J.L. Sessler, Jonathan L. Sessler, Q. He, *Coord. Chem. Rev.* 425 (2020) 213528.
- [23] N. Song, T. Kakuta, T.A. Yamagishi, Y.W. Yang, T. Ogoshi, *Chem* 4 (2018) 1–25.
- [24] T. Kakuta, T.A. Yamagishi, T. Ogoshi, *Acc. Chem. Res.* 51 (2018) 1656–1666.
- [25] F. Diederich, *Angew. Chem. Int. Ed.* 27 (1988) 362–386.
- [26] Z. Liu, S.K.M. Nalluri, J.F. Stoddart, *Chem. Soc. Rev.* 46 (2017) 2459.
- [27] J. Lagona, P. Mukhopadhyay, S. Chakrabarti, L. Isaacs, *Angew. Chem. Int. Ed.* 44 (2005) 4844.
- [28] V.N. Vukotic, S.J. Loebet, *Chem. Soc. Rev.* 41 (2012) 5896–5906.
- [29] H.T. Feng, Y.X. Yuan, J.B. Xiong, Y.S. Zheng, B.Z. Tang, *Chem. Soc. Rev.* 47 (2018) 7452–7476.
- [30] D. Zhang, A. Martinez, J.P. Dutasta, *Chem. Rev.* 117 (2017) 4900–4942.
- [31] T.J. Mooibroek, J.M. Casas-Solvas, R.L. Harniman, et al., *Nat. Chem.* 8 (2016) 69–74.
- [32] E.J. Dale, N.A. Vermeulen, A.A. Thomas, et al., *J. Am. Chem. Soc.* 136 (2014) 10669–10682.
- [33] S.C. Bete, M. Otte, *Angew. Chem. Int. Ed.* 60 (2021) 18582–18586.
- [34] L.X. Cai, S.C. Li, D.N. Yan, et al., *J. Am. Chem. Soc.* 140 (2018) 4869–4876.
- [35] C. Zhang, Z. Wang, L.X. Tan, et al., *Angew. Chem. Int. Ed.* 54 (2015) 9244–9248.
- [36] T. Jiao, L. Chen, D. Yang, et al., *Angew. Chem. Int. Ed.* 56 (2017) 14545–14550.
- [37] M.T. Nguyen, M.D. Krzyaniak, M. Owczarek, et al., *Angew. Chem. Int. Ed.* 56 (2017) 5795–5800.
- [38] W.W. Porter, T.P. Vaid, A.L. Rheingold, *J. Am. Chem. Soc.* 127 (2005) 16559–16566.
- [39] C. Cheng, P.R. McGonigal, S.T. Schneebeli, et al., *Nat. Nanotechnol.* 10 (2015) 547–553.
- [40] H.P. Chen, X.P. Liu, Y. Dou, et al., *Biomaterials* 34 (2013) 4159.
- [41] L.Z. Ma, T.F. Yang, Z.Y. Zhang, et al., *Chin. Chem. Lett.* 30 (2019) 1942–1946.
- [42] M.E. Brewster, T. Loftsson, *Adv. Drug Delivery Rev.* 59 (2007) 645–666.
- [43] J. Li, X.J. Loh, *Adv. Drug Delivery Rev.* 60 (2008) 1000–1017.
- [44] J.X. Zhang, P.X. Ma, *Adv. Drug Delivery Rev.* 65 (2013) 1215–1233.
- [45] H. Kitagishi, S. Hatada, T. Itakura, et al., *Org. Biomol. Chem.* 11 (2013) 3203.
- [46] K. Liu, Y.L. Liu, Y.X. Yao, et al., *Angew. Chem. Int. Ed.* 125 (2013) 8443–8447.
- [47] Y.M. Zhang, Q.Y. Xu, Y. Liu, *Sci. China Chem.* 62 (2019) 549–560.
- [48] Y.W. Li, Y.H. Dong, X.R. Miao, et al., *Angew. Chem. Int. Ed.* 57 (2018) 729–733.
- [49] Y.W. Li, Y.H. Dong, L. Cheng, et al., *J. Am. Chem. Soc.* 141 (2019) 8412–8415.
- [50] Y.W. Li, Q.F. Li, X.R. Miao, et al., *Angew. Chem. Int. Ed.* 60 (2021) 6744–6751.
- [51] H.T. Feng, J.W.Y. Lam, B.Z. Tang, *Coord. Chem. Rev.* 406 (2020) 213142–213155.
- [52] H.H. Duan, Y.W. Li, Q.F. Li, et al., *Angew. Chem. Int. Ed.* 59 (2020) 10101–10110.
- [53] H.H. Duan, F. Cao, H.X. Hao, H.T. Bian, L.P. Cao, *ACS Appl. Mater. Interfaces* 13 (2021) 16837–16845.
- [54] W.J. Xu, H.H. Duan, X.M. Chang, et al., *Sens. Actuators B: Chem.* 340 (2021) 129916.
- [55] Y.W. Li, C.Y. Qin, Q.F. Li, et al., *Adv. Opt. Mater.* 8 (2020) 1902154.
- [56] L. Cheng, H.Y. Zhang, Y.H. Dong, et al., *Chem. Commun.* 55 (2019) 2372–2375.
- [57] L. Cheng, K. Liu, Y.J. Duan, et al., *CCS Chem.* 2 (2020) 2749–2751.
- [58] H. Nian, A.S. Li, Y.W. Li, et al., *Chem. Commun.* 56 (2020) 3195–3198.
- [59] C.Y. Qin, Y.W. Li, Q.F. Li, et al., *Chin. Chem. Lett.* 32 (2021) 3531–3534.
- [60] P.P. Neelakandan, M. Hariharan, D. Ramaiah, *J. Am. Chem. Soc.* 128 (2006) 11334–11335.
- [61] P.P. Neelakandan, P.C. Nandajan, B. Subymol, D. Ramaiah, *Org. Biomol. Chem.* 9 (2011) 1021–1029.
- [62] P.P. Neelakandan, D. Ramaiah, *Angew. Chem. Int. Ed.* 47 (2008) 8407–8411.